ChalcogenideLetters Vol. 7, No. 12, December 2010, p 641-646

OPTICAL AND STRUCTURAL CHARACTERIZATION OF AIR-ANNEALED CdS FILM PREPARED BY CHEMICAL BATH DEPOSITION (CBD) TECHNIQUE

ATEFEH JAFARI[a], ZAHID RIZWAN[a], MOHD SABRI MOHD GHAZALI[a], FASIH UD DIN[a], AZMI ZAKARIA[a, b*]

[a]*Department of Physics, Faculty of Science, Universiti Putra Malaysia, 43400 Serdang, Selangor D.E., Malaysia*

[b]*Advanced Material and Nanotechnology Laboratory, Institute of Advanced Technology, Universiti Putra Malaysia, 43400 UPM Serdang, Selangor D.E., Malaysia*

The $CdCl_2$ and $(NH_2)_2CS$ were used to prepare CdS thin films, to be deposited, on glass substrate by chemical bath deposition (CBD) technique employing $CdCl_2$ (0.005 M) and $NH_2)_2CS$ (0.01 M) as a source of Cd^{2+} and S^{2-}, respectively at constant bath temperature 70 ^oC. The films were air-annealed at 200 to 360 ^oC for 1 hour. XRD analyses reveal that the films were cubic along with two feeble peaks of orthorhombic $CdSO_4$ at the annealing temperature 320 and 360 ^oC. The crystallite size of the films was increased from 59.2 to 67 nm with the increase of annealing temperature. Optical energy band gap (E_g) and absorption coefficient (α) were chosen as parameters of characterization, calculated from the transmission spectral data and were discussed as function of annealing temperature.

(Received November 29, 3010; accepted December 7, 2010)

Keywords: CBD, CdS, Thin films, Air-annealing

1. Introduction

Techniques like electro-deposition, vacuum evaporation, sputtering, radio frequency, pulsed laser evaporation, MBE, (MOCVD), SPD, CSS, SILAR, Micelle method and chemical bath deposition (CBD) are being used to develop thin films. Among these techniques, chemical bath deposition (CBD) has become an attractive route due to its simplicity, being inexpensive and having large surface area deposition at low temperature. It is being used to grow CdS films since 1960s [1-3]. CBD technique also enhances the performance of CdS window layer. The films deposited by CBD are composed of closely packed nanocrystals (NCs) which make them attractive for basic and applied research of NCs [4]. The highest efficiency was obtained with the use of CBD to deposit thin films of CdS as a window and buffer layer to grow the CdTe and CIGS solar cells [5-8]. CdS is an excellent hetrojunction partner for p-type CdTe, $CuInSe_2$, $Cu(In,Ga)Se_2$ (CIGS) because of the wide optical band gap (2.42 eV). CdS is also important material due to its novel properties like photoconductivity, high index of refraction (2.5) and its high electron affinity [9, 10]. The substrate is immersed in a bath of alkaline aqueous solution having Cd^{2+} and S^{2-} resulting from the chemical reaction in the solution to deposit CdS film on the immersed substrate [11-13]. In this study, CBD technique has been used to deposit nanostructured CdS thin films on glass slides at the solutions concentration of $CdCl_2$ [0.005 M] and $(NH_2)_2CS$ [0.01 M]. Optical and structural properties of CdS films are discussed as a function of annealing temperature.

*Corresponding author: azmizak@gmail.com

2. Experimental

All the reagents and solvents used were of analytical grade (99.9 % pure, Alfa Aesar). $CdCl_2$ and $(NH_2)_2CS$ were used to grow CdS films on commercial glass slides (76 × 25 × 1.2 mm) as substrate. The substrates were cleaned in acetone and ethanol ultrasonically for 30 minutes. Then substrates were washed with deionized water and dried under N_2 atmosphere. Solution of $CdCl_2$ [0.005 M] and $(NH_2)_2CS$ [0.01 M] were prepared in doubly distilled deionized water by continuous stirring at room temperature. $CdCl_2$ and $(NH_2)_2CS$ solutions were placed separately in water bath using digital hot plate and temperature was raised upto 65 ^oC while stirring. Ammonia (NH_3) in aqueous solution was used as a complexing agent. Aqueous NH_3 was added drop by drop in $CdCl_2$ solution to dissolve white precipitates of $Cd(OH)_2$ under stirring conditions. pH of the solution was adjusted at 11. Thiourea solution was added in $CdCl_2$ solution in 30 seconds under vigorous stirring. The temperature of resulting clear solution was further raised to 70 ^oC. Six cleaned substrates were immersed vertically in the solution using special holders under stirring condition. The container was covered to avoid the evaporation of ammonia. Mercury thermometer was also used to countercheck the temperature variations of the solution. Substrates were taken out from water bath after 2 hours deposition time. Deposited substrates were washed in deionized water ultrasonically to remove the loosely adhered CdS particles and were dried at ambient conditions. Deposited film samples were divided into six sets. One of the six samples was characterized as-deposited A_0. Other samples were air-annealed in the temperature range (200 - 360 ^oC) for 1 h at a heating and cooling rate of 4 ^oC min^{-1}. Air- annealed samples were characterized for the annealing temperature 200 ^oC (A_{200}), 240 ^oC (A_{240}), 280 ^oC (A_{280}), 320 ^oC (A_{320}) and 360 ^oC (A_{360}). Thickness of the films was measured by Ellipsometer. Cu K_α radiation (λ = 1.540598 Å) with PANalytical (Philips) X'Pert Pro PW1830 was used for XRD analysis. The XRD data were analyzed by X'Pert High Score software for the identification of the crystalline phases in the films. Crystallite size (D) was determined using Scherer formula,

$$D = \frac{K(\lambda)}{\beta\cos\theta} \tag{1}$$

where β is the full width at half maximum (FWHM in radians) of the x-ray diffracted peak corrected for instrumental broadening and θ is Bragg angle, λ is the wavelength of X-ray, K is Scherer constant; taken as 0.94 for the calculations [14, 15].

The optical transmission (T) data was measured by double beam spectrophotometer (Shimadzu) over the wavelength range of 350 to 1100 nm. The absorption coefficient (α) was calculated using the equation,

$$\alpha = \frac{\mathrm{Ln}\left(\frac{1}{T}\right)}{d} \tag{2}$$

Optical energy band gap (E_g) can be calculated using absorption coefficient (α),

$$\alpha = \frac{A\left[(hv - E_g)\right]^n}{hv} \tag{3}$$

where A is constant, hv is photon energy, n is ½ for direct band gap materials as CdS is a direct band gap material [16, 17]. $(\alpha hv)^2$ is plotted as a function of hv. The linear portion of the curve extrapolated to $(\alpha hv)^2 = 0$, gives the value of E_g.

3. Results and discussion

CdS films prepared from a reaction mixture containing cadmium chloride and thiourea show polycrystalline nature [18, 19] as shown in XRD pattern (Fig. 1). The XRD graphs are scaled to a small size and six graphs are given in one figure, many of the small peaks are lost in this process. Here, all of the peaks observed are described in detail. Peaks observed for the sample A_0 at 2θ = 26.7552°, 30.3602°, 44.2177°, 52.3606°, 55.0631°, 70.7554° and 72.9154° (ref: 01-080-0019) belong to (111), (200), (220), (311), (222), (331), (420) cubic CdS, respectively. Peaks are observed for the sample A_{200} at 2θ = 26.7674°, 30.4024°, 44.3195°, 52.4880°, 54.8619°, 70.7788°

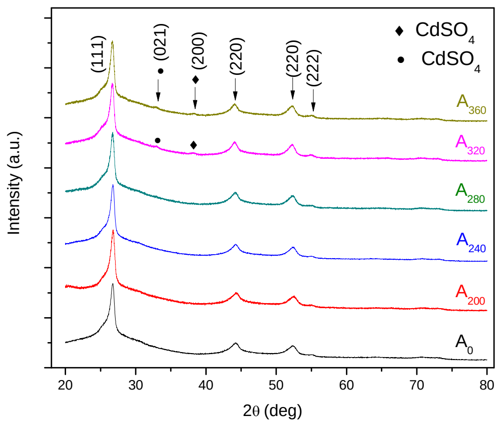

Fig. 1: XRD pattern of CdS film at different annealing temperatures

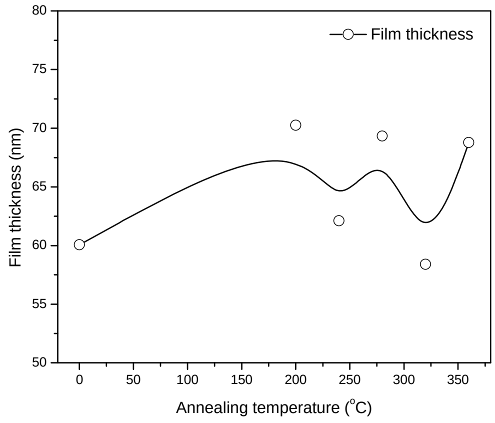

Fig. 2: Variation of CdS film thickness with annealing temperature

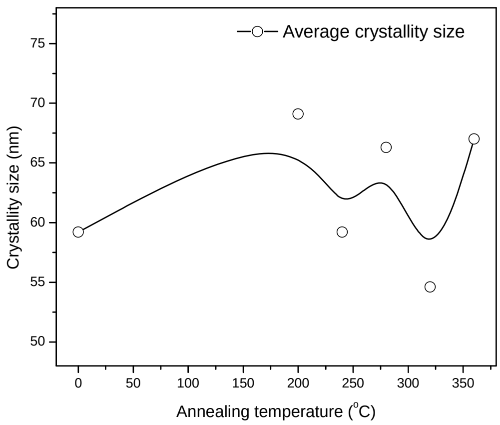

Fig. 3: Variation of crystallite size with annealing temperature

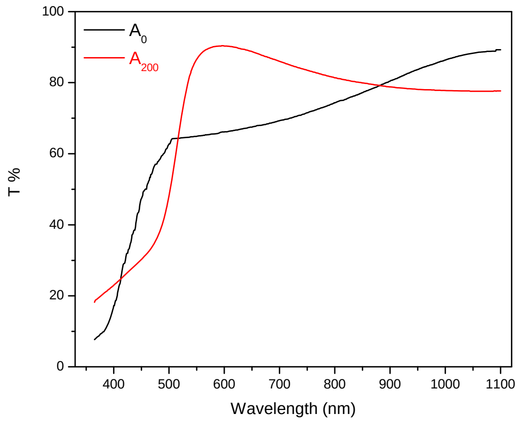

Fig. 4: Transmittance spectra for as-deposited (A_0) and annealed at 200 ^{0}C (A_{200})

and 73.1410° (ref. 01-075-0581) belong to (111), (200), (220), (311), (222), (331) and (420) cubic CdS phase, respectively [20]. Peaks are observed for the sample A_{240} at 2θ = 26.7606°, 30.4136°, 44.2088°, 52.3975°, 54.9751° and 73.1410° (ref. 01-075-1546) belong to (111), (200), (220), (311), (222), (331) and (420) cubic CdS phase, respectively. The observed peaks for the sample A_{280} are at 2θ = 26.8924°, 30.4377°, 44.1860°, 52.3839°, 54.9199° and 72.8630° (ref. 00-042-1411) belongs to (111), (200), (220), (311), (222) and (420) cubic CdS phase, respectively. The sample A_{320} have peaks at 2θ = 26.5762°, 44.0994°, 52.2651°, 54.9215° and 72.7985° (ref. 01-075-0581) belong to (111), (220), (311), (222) and (420) cubic CdS phase, respectively. Two very small peaks are also observed at 2θ = 32.8988° and 38.1316° (ref. 00-014-0352) which belong to (021) and (200) orthorhombic $CdSO_4$ phase. Peaks are observed for the sample A_{360} at 2θ = 26.7241°, 44.0729°, 52.4358°, 55.01714° and 72.7864° (ref. 01-075-0581) belong to (111), (220), (311), (222) and (420) cubic CdS phase, respectively. Two very small peaks are also observed at 2θ = 32.8076° and 38.1961° (ref. 00-014-0352) which belong to (021) and (200) orthorhombic $CdSO_4$ phase. It is observed that the only two very small peaks of secondary phase i.e $CdSO_4$ appeared at the annealing temperature 320 and 360 °C. The relative percentage error in standard ‘d’ value (3.35498, ref: 01-080-0019) and observed ‘d’ value is below 0.6 %. It is also observed that the preferred orientation in the deposited CdS films is (111). The preferred orientation (111) is due to the controlled nucleation process occurring in the deposited films. This suggests the slow growth rate of the film deposition [21]. Thickness of the film sample A_0 is 60.1 nm and is further increased with the increase of the annealing temperature (Fig. 2). Thickness is about 70.2 nm for the sample A_{200} and is further decreased to 62.1 nm at the annealing temperature 240 °C. The minimum thickness i.e. 58.4 nm, is obtained at the 320 °C annealing temperature. The average crystallite size of the film sample A_0 is 59.2 nm. The crystallite size of the sample A_{200} is 69.1 nm and is further reduced to 59.2 nm for the sample A_{240} (Fig. 3). The minimum crystallite size i.e. 54.06 nm, is obtained at the 320 °C annealing temperature. It is observed the thickness and particle size has the same trend with the increase of the annealing temperature (Fig. 2 and 3).

The transmittance spectra of CdS films are recorded over 350 to 1100 nm (Fig. 4 to 7). The spectra showed transmittance dependence of film on the wavelength at the different annealing temperatures. The transmittance is 62.7% at wavelength of 500 nm for sample A_0 (as deposited)

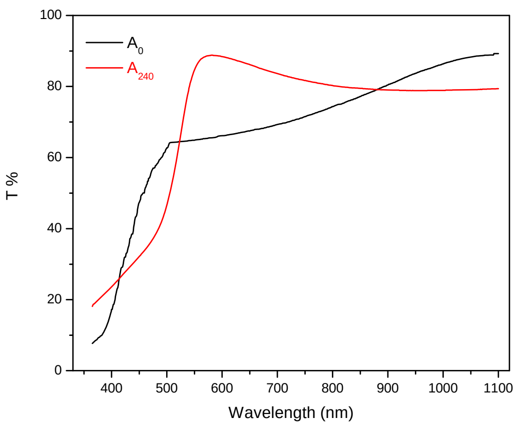

Fig. 5: Transmittance spectra for as-deposited (A_0) and annealed at 240 ^{0}C (A_{240})

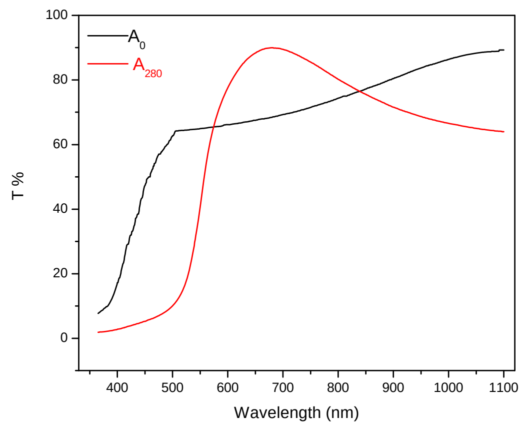

Fig. 6: Transmittance spectra for as-deposited (A_0) and annealed at 280 ^{0}C (A_{280})

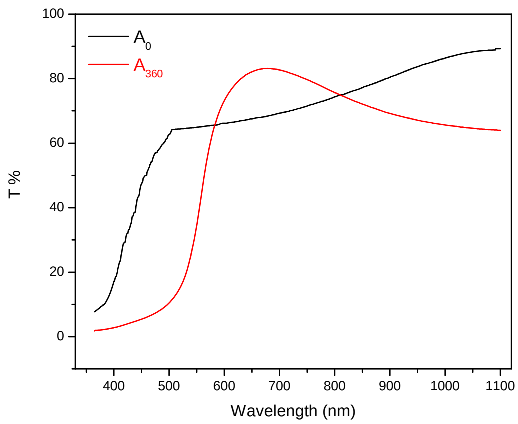

Fig. 7: Transmittance spectra for as-deposited (A_0) and annealed at 360 ^{0}C (A_{360})

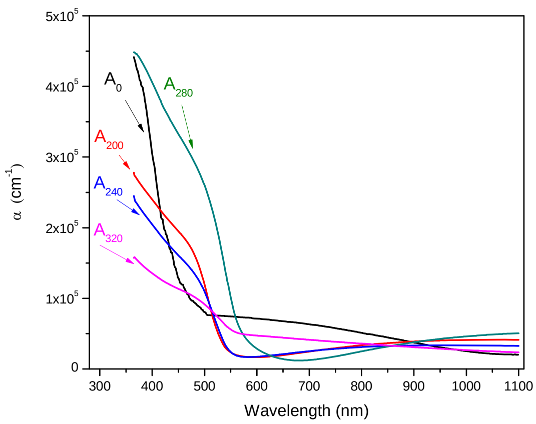

Fig. 8: Variation of absorption coefficient (α) with wavelength at different annealing temperatures

and is increased to 77% at the wavelength 850 nm (Fig. 4). It is increased to 89 % with the further increase of wavelength. The transmittance is about 48% at wavelength of 500 nm for the sample A_{200} and is increased sharply to 90% at the wavelength 600 nm (Fig. 4). It is further decreased to 77% with the increase of wavelength. It is observed that the spectrum shifted towards higher wavelength [22]. This suggests the decrease in optical energy band gap (E_g) with the annealing temperature as shown in the (Fig. 10). This indicates the increase in the crystallinity. The transmittance is 47% at wavelength of 500 nm for the sample A_{240} and is increased sharply to 89% at the wavelength 600 nm (Fig. 5). It is further decreased to 80% with the increase of wavelength. It is observed that the spectrum shifted towards higher wavelength. This suggests the decrease in optical energy band gap (E_g) with the annealing temperature as shown in the (Fig. 10). This indicates the increase in the crystallinity with the annealing at 240 ^{o}C. The transmittance is 11% at wavelength of 500 nm for the sample A_{280} and is increased sharply to 91% at the wavelength 680 nm. It is further decreased to 64% with the increase of wavelength (Fig. 6). It is observed that the spectrum shifted towards higher wavelength. This suggests the decrease in optical energy band gap (E_g) with the annealing temperature as shown in the (Fig. 10). This indicates the increase in the crystallinity with the annealing at 280 ^{o}C. The transmittance is 12% at wavelength of 500 nm for the sample A_{360} and is increased sharply to 83% at the wavelength 660 nm, It is further decreased to 64% with the increase of wavelength (Fig. 7). It is observed that the spectrum shifted towards higher wavelength. This suggests the decrease in the E_g with the annealing temperature (Fig. 10). This indicates the increase in the crystallinity at the annealing at 360 ^{o}C. The best transmittance is obtained at the annealing temperature 200 ^{o}C for this chemical bath conditions. The variation of the optical absorption coefficient (α) with the wavelength is shown in the Fig. 8.

The graph $(\alpha h\nu)^2$ versus photon energy ($h\nu$) (Fig. 9). The value of the E_g is 2.85 eV for sample A_0. The value of the E_g is reduced to 2.50 eV for sample A_{200}. It is observed that there is a prominent change in the value of E_g for the samples A_0 and A_{200} (Fig. 10). This suggests that the crystallinity of the films is increased with the annealing temperature. It is clear from Fig. 2 that the film thickness is also increased with the increase of annealing temperature. Particle size also increased with the increase of annealing temperature. This suggests the crystallinity increases with the annealing temperature. It is observed the trend in the change of E_g, film thickness and particle size is same with the increase of annealing temperature.

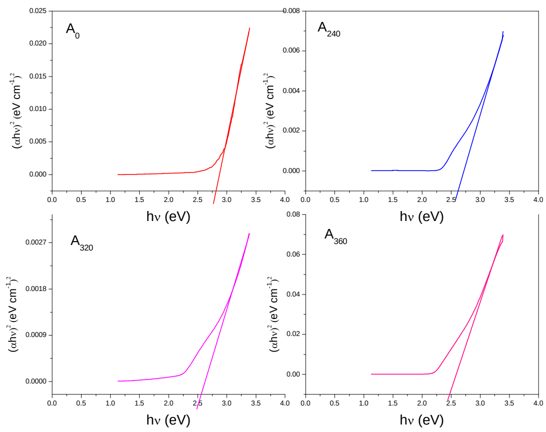

Fig. 9: Variation of E_g with hυ at different annealing temperatures

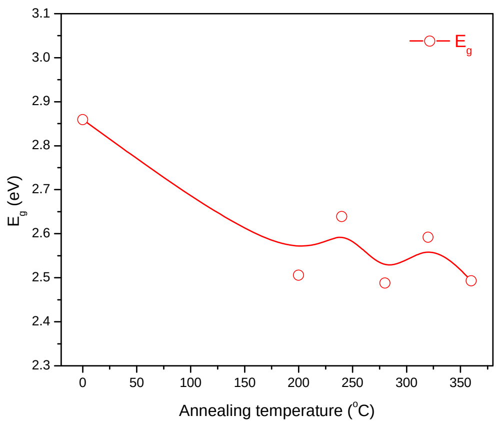

Fig. 10: Variation of E_g with annealing temperature

4. Conclusions

The CdS films were deposited by CBD technique for the different solution concentrations at constant bath temperature. XRD analysis showed that the films were in cubic phase along with two very small peaks of orthorhombic $CdSO_4$ at the annealing temperature 320 and 360 ^oC. The crystallite size was varied with the annealing temperature. The value of optical band gap of the as-deposited film was 2.85 eV and decreased to 2.49 eV at the annealing temperature 360 ^oC. The best optical transmittance was observed at the annealing temperature 200 ^oC.

Acknowledgement

The authors are thankful to the Malaysian Ministry of Higher Education for funding this research work through FRGS Project # 01-01-07-139FR

References

[1] S. Mokrushin, Y. Tkachev, Colloid J. USSR, , **23**, 366 (1961)
[2] G. Kitaev, A. Uritskaya, S. Mokrushin, Russ. J. Phys.Chem., **39**, 1101 (1965)
[3] J. Zhang, L. Sun, S. Liao, C. Yan, Solid State Communication, **124**(1-2), 45 (2002)
[4**]** G. Hodes, A. Albu-Yaron, F. Decker, P. Motisuke, Phys.Rev.B, **36**, 4215 (1987)
[5] B. Contreras, Egaas, K. Ramanathan, J. Hiltner, A. Swartzlander, F. Hasoon, R. Noufi, Prog. Photovolt, Res. Appl., **7**(4), 311 (1999)
[6] H. Khallif, I. O. Oladej, L. Chow, Thin Solid Films, **516**, 5967 (2008)
[7] I. Oladeji, L. Chow, C. Ferekides, V. Viswanathan, Z. Zhao, Sol. Energy Mater. Sol. Cells, **61**(2), 203 (2000)
[8] M. Contreras, M. Romero, B. To, F. Hasoon, R. Noufi, S. Ward, K. Ramanathan, Thin Solid Films, **403/404**, 204 (2002)
[9] T. L. Chu, S. S. Chu, C. Ferekides, C. Q. Wu, J. Britt, C. Wang, J. Cryst. Growth, **117** (1-4), 1073 (1992)
[10] C. Ferekides, J. Britt, Sol. Energy Mat. Sol. Cells, **35**, 255 (1994)
[11] I. Kaur, D. K. Pandya, L. Chopra, J. Electrochem. Soc., **127**(4), 943 (1980)
[12] M. Froment, D. Lincot, Electrochim. Acta, **40**(10), 1293 (1995)
[13] C. Voss, Y. J. Chang, S. Subramanian, S.O. Ryu, T.J. Lee, C.H. Chang, J. Electochem, Soc., 151 (**10**), C 655 (2004)
[14] M. Caglar, Y. Caglar, S. Ilican, J. Optoelectron. Adv. Mater., **8** (4), 1410 (2006)
[15] S. Prabahar, M. Dhanam, J. Crys. Growth, **285**, 41 (2005)
[16] V. B. Sanap, B. H. Pawar, Chalcogenide Lett., **7** (3), 223 (2010)
[17] M. V. Kurik, Phys. Status Solidi (a), **8**(1), 9 (1971)
[18] K. R. Murali, M. Matheline, R. John, Chalcogenide Lett., **6** (9), 483 (2009)
[19] S. Soundswarm, O. S. Kumar, R. Dhanasekaran, Mater.Lett., **58**, 2381 (2004)
[20] G. C. Morris, R. Vanderveen, Sol. Energy Mater. Sol. Cells, **27**(4), 305 (1992)
[21] G. Sasikala, P. Thilakan, C.Subramanian, Sol. Energ. Mater. Sol. Cells., **62**, 275 (2000)
[22] F. Liu, Y. Lai,. J. Liu, B. Wang, S. Kuang, Z. Zhang, J. Li, Y. Liu, J. Alloy. Compd., **493**, 305 (2010)

\